Optics Communications 479 (2021) 126457

Contents lists available at ScienceDirect

Optics Communications

journal homepage: www.elsevier.com/locate/optcom

The role of metastable atoms in atomic excitation process of magnesium in microwave-assisted laser plasma

Ali Khumaeni [a,*], Katsuaki Akaoka [b], Masabumi Miyabe [b], Ikuo Wakaida [b]

[a] Department of Physics, Faculty of Science and Mathematics, Diponegoro University, Tembalang 50275, Semarang, Indonesia
[b] Remote Analytical Technology Group, Collaborative Laboratory for Advanced Decommissioning Science, Japan Atomic Energy Agency, Shirakata 2-4, Tokai-mura, Naka-gun, Ibaraki-ken, 319-1195, Japan

ARTICLE INFO

Keywords:
Laser induced breakdown spectroscopy
Metastable He atoms
LIBS
Nd:YAG laser
Excitation process

ABSTRACT

Study on the excitation process of magnesium atom has been conducted in microwave-assisted laser plasma. Experimentally, an Nd:YAG laser (532 nm, 5 mJ) was directed into the magnesium oxide (MgO) sample in various gases of helium, argon, and air at a reduced pressure to induce a luminous plasma. The plasma emission was significantly enhanced when a microwave (2.45 GHz, 400 W) was introduced into the laser plasma. Results revealed that the emission intensity of the ionic magnesium lines that have relatively low excitation energy (around 4 eV) is high only in helium and argon ambient gases. On the contrary, the intensity of ionic magnesium lines having high excitation energy (8–11 eV) is high only for helium gas. The results suggested that a particular excitation process takes place in the microwave-assisted laser plasma induced in helium and argon gases, namely the excitation mechanism proceeds through metastable atoms overwhelmingly produced in the microwave-assisted laser-induced plasma.

1. Introduction

Laser-induced breakdown spectroscopy (LIBS) is a powerful optical emission spectroscopy technique for qualitative and quantitative elemental analysis in various phases including liquids, solids, and gases [1–7]. In conventional LIBS, a pulse laser source is employed to vaporize, atomize and excite a sample forming a luminous plasma. LIBS has several advantages including no need of sample preparation, the possibility of in situ analysis, and the capability of micro-area analysis [8–10]. This technique has been applied in various applications including biological identification [11–13], biomedical applications such as human blood analysis [14–16], material analysis [17–20], environmental monitoring [21–24], forensic [25–27], and space exploration [28–30]. Even though rapid analysis can be realized, LIBS still suffers from low limit of detection compared to other analytical techniques such as inductively coupled plasma atomic emission spectroscopy [31,32].

To overcome the problems, researchers suggested and developed double pulse LIBS (DP-LIBS) by employing second pulse laser to enhance the plasma emission using colinear double pulse and orthogonal double pulse [33–36]. Significant increment in signal to noise ratio (S/N ratio) and emission intensity were obtained compared to the case of single pulse laser (standard LIBS). In DP-LIBS, first pulse laser is generally used to initiate first target ablation, followed by the second laser to reheat the ablated atoms. The role of re-excitation by the second pulse laser in the enhancement of emission intensities was suggested by some researchers [37–39]. The others urged the large mass removal in DP-LIBS plays a role in the intensity enhancement [40–42].

In other direction, some researchers applied a microwave for the enhancement of laser plasma emission. Generally, this technique referred to as microwave-assisted laser-induced breakdown spectroscopy (MA-LIBS). Envimetrics and Liu et al. applied microwave to enhance the plasma emission of the metal samples [43,44]. Kearton et al. and Y. Liu et al. reported intensity enhancements by using laser-assisted microwave spectroscopy (LAMPS) [45,46]. Ikeda et al. used microwave to extend the lifetime of plasma emission to millisecond [47,48]. However, in the methods, waveguides and microwave cavity were required.

For the convenience application of microwave, we developed a novel method of microwave-assisted LIBS (MA-LIBS) coupled by an antenna for the enhancement of LIBS emission [49]. In this method, a luminous plasma is induced by a low energy of pulsed laser at a local point, at which electromagnetic field was produced by localizing microwave radiation. A microwave (MW) is applied through an antenna via coaxial cable to enhance the plasma emission. This present method is very potential to be used for the enhancement of emission intensity of elements, which enables us to improve the sensitivity of analytical results, and for the selection of high resolution spectrometer for the analysis of complex spectral lines, such as nuclear fuel spectrum.

* Corresponding author.
E-mail address: khumaeni@fisika.fsm.undip.ac.id (A. Khumaeni).

https://doi.org/10.1016/j.optcom.2020.126457
Received 7 May 2020; Received in revised form 26 August 2020; Accepted 12 September 2020
Available online 14 September 2020

In addition to DP-LIBS and MA-LIBS, atmospheric condition such gas composition and ambient pressure also gives influence to the observed emission intensity [50,51]. Iida et al. reported that the He and Ar ambient gases are useful in increasing LIBS emission intensity compared to ambient air. Heavier ambient gases cause slow plasma expansion, resulting in shorter plasma length and lifetime [52]. Also, the ambient gases affect the ablation rate in the order He>Ne>air>Ar as reported by Sdorra and Niemax [53]. Idris et al. performed analysis of carbon using LIBS in He gas and air at low pressure condition [54]. Significant enhancement of signal intensity was obtained in He environment compared to air, which is explained by the role of He metastable atoms in the excitation process. The role of He metastable atoms to produce excellent spectral quality was also reported by Hedwig et al. in the food analysis using standard nanosecond LIBS [55]. They suggested that the He metastable atoms play an important role in the excitation process. We have also studied the excitation mechanism of Ca and Mg atoms in various gases including He gas and air, and concluded that the excitation process of atoms in He gas takes place via metastable atoms through penning effect as reported here [56].

In this present work, the role of ambient gases in the enhancement of plasma emission in MA-LIBS was investigated. The mechanisms by which the ambient conditions affect MA-LIBS emission have been presented. Helium, argon, and air at pressure ranging from 0.6 to 12 kPa are used to examine the effect of ambient conditions on the plasma emission. The result certified that metastable atoms play an important role in the excitation process especially in He and Ar environment.

2. Experimental procedure

The experimental setup used in this research is shown in Fig. 1. A second-order harmonic of Q-switched Nd:YAG laser (Quanta-Ray, Spectra Physics, 532 nm, 8 ns) was directly focused onto a sample surface through a quartz window using quartz lens with a focal length of 200 mm. During the experiment, the laser energy was varied from 5 mJ to 60 mJ by using a polarizer and a filter. The laser plasma was enhanced by intensified microwave field induced with an antenna; the antenna was circular shaped with a diameter of 3 mm. As described in our previous work [49], by using antennas with a different diameter (3 mm and 9 mm), we experimentally proved that the optimum enhancement of emission intensity was obtained when the diameter of 3 mm was used. Microwave was generated by using a magnetron at a frequency of 2.45 GHz (MUEGGE MG0500D-215TC, 0–1 ms). The power of the magnetron was varied from 100 W to 400 W. The Nd:YAG laser and microwave were operated in the synchronization mode with a delay time of 10 μs for the Nd:YAG laser bombardment relative to the microwave generation; Namely, the Nd:YAG laser was bombarded on sample target 10 μs after microwave generation. For a comparative study, we also used standard LIBS without microwave. In this experiment, pulse Nd:YAG laser with an energy of 5 mJ was employed as an energy source.

The sample used in the experiments was magnesium oxide (MgO) pellet. The sample is 1 mm thick and 10 mm in diameter. The sample was made by compressing MgO powder of 0.5 g by the pressure of 1.5 MPa.

During the experiment, the sample was placed in a metal chamber equipped by windows, on which the fine gold mesh (lattice constant of 100 μm and wire diameter of 30 μm) was attached. The chamber functioned to block the microwave radiation. The pressure of the surrounding gas in the chamber was set at various reduced pressure from 0.26 to 12 kPa. During the experiment, various ambient gases including helium, argon, air were flowed.

The emission spectrum was obtained by using an ICCD camera (Andor, iStar) through a high-resolution echelle spectrometer (ARYELLE) with the resolution of 50 pm at the wavelength of 360–460 nm. The light emission of the laser plasma was collected by using an optical fiber, which fed into the spectrometer. The plasma radiation at 2–5 mm from the sample surface was imaged in a ratio of 1:1 onto one end of the fiber by using a quartz lens (f= 100 mm).

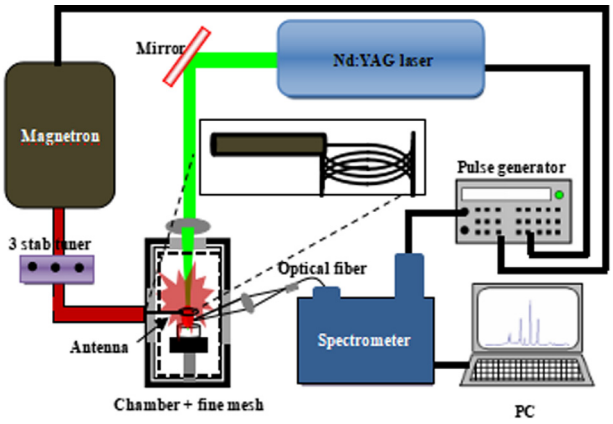

Fig. 1. Experimental setup used in this work.

3. Results and discussion

As reported in our previous work [49], the enhancement of LIBS plasma emission occurs when the microwave coupled by a loop antenna was introduced into the LIBS plasma. In this work, the role of ambient gases in the enhancement of plasma emission in MA-LIBS was investigated.

Fig. 2 shows a comparison of integrated emission spectra of magnesium taken from the magnesium oxide sample in the wavelength region of 275–300 nm by using LIBS (dashed blue line) and MA-LIBS (red line) in (a) helium gas, (b) argon gas, and (c) air. The spectra were taken at a reduced pressure of 1.3 kPa. The laser energy and microwave power were 5 mJ and 400 W, respectively. The spectra were accumulated for 30 pulses for both microwaves on and off, with each laser shot hits at a fresh point of the moving sample surface to avoid shot-to-shot fluctuation. For data acquisition in conventional LIBS, the gate delay time and gate width of spectrometer were 2 μs and 600 μs, respectively, while for MA-LIBS case, the data acquisition started at 2 μs after laser bombardment and the gate width of spectrometer was also set at 600 μs. It is seen in Fig. 2 that regardless of gas kinds, the background intensity in the emission spectra is almost negligible. However, in argon gas and air, the spectra of LIBS emission relatively noisy compared to the case of helium gas. The emission intensity of neutral and ionic Mg lines (blue dotted line) is relatively weak for the conventional LIBS in all gases. The intensity (red line) significantly enhanced when the intensified microwave was injected into the LIBS plasma. The enhancement was defined as the ratio between the MA-LIBS intensity and LIBS intensity after subtracting background emission as defined also in our previous paper [49]. Based on this definition, it is obtained that the enhancement happens for all neutral and ionic Mg emission lines and their enhancement varies in all gases including He, Ar, and ambient air. For example, enhancement of ionic Mg II 280.3 nm emission intensity for helium gas, argon gas, and air is approximately 350, 860, and 600 times as shown in Figs. 2(a), 2(b), and 2(c), respectively. Furthermore, the enhancement of Mg II 279.6 nm in all gases is also relatively high. Namely, the enhancements are 660, 105, and 125 in He, Ar, and ambient air, respectively. However, it should be emphasized that the emission intensities of Mg ionic line that have a high excitation energy (~9 eV), namely Mg II 279.8 nm, Mg II 292.9 nm, Mg II 293.7 nm can clearly be observed only for the case of He surrounding gas [Fig. 2(a)] and they are faintly detected in the argon and air plasmas [Figs. 2(b) and 2(c)].

Table 1 summarizes the observed emission lines of Mg along with their spectroscopic parameters, taken from the Kurucz and NIST atomic database [57,58], and their intensities. As indicated in Table 1, the excitation energy of Mg II 279.6 nm and Mg II 280.3 nm are 4.4 eV and 4.4 eV, respectively; Mg II 279.8 nm is 8.9 eV; Mg II 292.9 nm

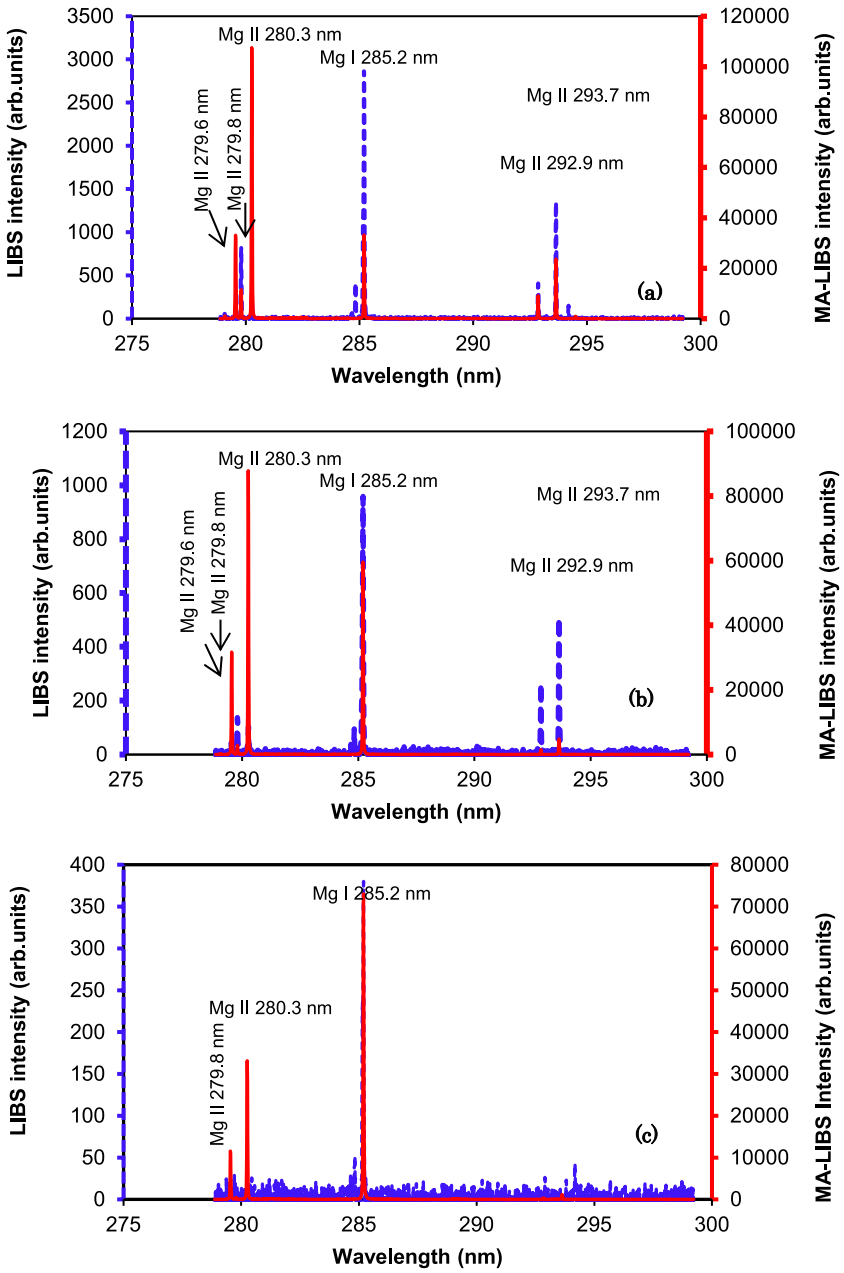

Fig. 2. Emission spectrum of magnesium taken from the magnesium oxide sample by using LIBS (dashed blue line) and MA-LIBS (red line) in (a) helium gas, (b) argon gas, and (c) air.. (For interpretation of the references to color in this figure legend, the reader is referred to the web version of this article.)

and Mg 293.7 nm have higher excitation energies of 8.7 eV; and Mg II 448.1 nm is 11.6 eV from the ground state of the Mg ion (Mg^{1+} ion). It is also observed that ionic Mg line with a high excitation energy (Mg II 448.1 nm) only clearly appears with relatively high intensity in the case of He gas and it is negligibly week intensity in argon gas and air (Table 1); the Mg II 448.1 nm has very high excitation energy of 11.6 eV from the ground state of the Mg ion (Mg^{1+} ion). It is probably difficult to excite atoms that have a high excitation energy. Larger emission intensity of ionic Mg lines that have a high excitation energy observed only in helium plasma interprets that there is any particular excitation process in laser plasma induced in helium environment.

To study in detail the excitation mechanism of atoms taking place in the microwave-assisted laser-induced plasma region, the effect of the ambient gas and the microwave radiation were studied. Two parameters including ambient gas pressure and time dependence were examined. First, we examined the effect of the ambient gas pressure on ionic Mg emission intensities in various surrounding gases obtained from the magnesium oxide sample taken by using laser plasma without microwave radiation (LIBS). For this purpose, ionic Mg emission lines having low ionic excitation energy of 4.4 eV (Mg II 280.3 nm) and ionic Mg lines having high excitation energy of 8.9 eV and 8.7 eV for Mg II 279.8 nm and Mg II 293.6 nm, and excitation energy of 11.6 eV (Mg II 448.1 nm) were used.

Fig. 3 displays how the ionic Mg emission intensities changes with the gas pressure for (a) Mg II 280.3 nm, (b) Mg II 279.8 nm, (c) Mg II 293.6 nm, and (d) Mg II 448.1 nm in various gases of He, Ar, and ambient air. It can clearly be seen that for all ionic Mg lines, the emission intensity peak occurs at a low pressure of around 0.27 to 0.67 kPa for Mg II 280.3 nm, Mg II 279.8 nm, Mg II 293.6 nm, and Mg II 448.1 nm in all various ambient gases. With increasing the ambient pressure, the emission intensity peaks decrease. This phenomenon also happens as reported by Bashir et al. and Knight et al. [59,60]. Namely, at lower ambient pressure, the laser plasma easily expands into the low-pressure region, which then reduces the density of the plasma constituent.

Table 1
Elements, wavelength, energy level, and transition probability for the neutral and ionic Mg emission lines used in this study.

Elements	Wavelength (nm)	Energy level (eV)		Transition probability (10^8)	Rel. Intensity (He)		Rel. Intensity (Ar)		Rel. Intensity (air)	
		Lower	Upper		LIBS	MA-LIBS	LIBS	MA-LIBS	LIBS	MA-LIBS
Mg I	277.669	2.7115918	7.175454	6.6	100	1400	100	1000	50	800
Mg I	277.827	2.7091048	7.170427	5.5	100	1000	100	900	50	700
Mg I	277.983	2.7115918	7.170427	4.1	550	4000	350	3200	200	2000
Mg I	278.128	2.7115918	7.167870	5.4	130	1200	50	800	50	600
Mg I	278.297	2.7166397	7.170427	6.4	190	1400	100	1000	50	700
Mg II	279.078	4.422431	8.863761	16.0	50	1000	–	200	–	–
Mg II	279.553	0	4.433784	10.4	50	33,000	300	32,000	20	2500
Mg II	279.799	4.433784	8.863654	28.7	840	11,000	–	3000	–	–
Mg II	280.270	0	4.422431	5.14	300	106,000	100	86,000	50	30,000
Mg I	285.212	0	4.345803	14.7	2850	33,000	950	60,000	380	73,000
Mg II	292.863	4.422431	8.654710	2.3	400	9000	250	1500	–	500
Mg II	293.651	4.433784	8.654710	4.6	1350	24,000	500	4800	–	500
Mg I	382.936	2.709105	5.945917	2.7	5550	8000	1300	13,000	1600	13,000
Mg I	383.230	2.711592	5.945917	2.0	1300	1500	300	2000	300	2000
Mg II	448.113	8.863654	11.62969	1.3	5600	19,000	60	1800	–	–
Mg I	517.268	2.711592	5.107827	1.0	3300	8300	500	15,000	800	17,500
Mg I	518.360	2.716639	5.107827	1.7	5100	11,000	600	20,500	1200	23,500

With decreasing the plasma density, the laser absorption via inverse Bremsstrahlung also decreases, decreasing the plasma shielding effect. The decreased plasma shielding effect allows more photons to reach the sample target, resulting in increased mass ablation of material target and finally increasing emission spectrum intensity. Once the ambient pressure increases, the plasma shielding effect also increases, retarding the photons to attain the sample target. Therefore, mass ablation of the target decreases, decreasing the spectrum intensity.

It should also be noticed that that the emission lines of Mg II 280.3 nm, Mg II 279.8 nm, Mg II 293.6 nm, and Mg II 448.1 nm has highest intensity for helium gas compared to the case of argon gas and ambient air as shown in Figs. 3(a), (b), (c), and (d), respectively. However, for argon gas, the emission intensities of ionic Mg II 280.3 nm, Mg II 279.8 nm, and Mg II 293.6 nm still clearly appear and it is very weak for ionic Mg II 448.1 nm. For ambient air case, all ionic Mg intensities are negligibly weak. As shown in Table 1, the Mg II 280.3 nm, Mg II 279.8 nm, Mg II 293.6 nm, and Mg II 448.1 nm have ionic excitation energy of 4.4 eV, 8.9 eV, 8.7 eV, and 11.6 eV, respectively, from the ground state of the Mg ion (Mg^{1+} ion = 7.6 eV). It is probably difficult to excite atoms that have a high excitation energy. The excitation process can take place only when the plasma temperature is very high. This implies that the excitation process in the air case proceeds through thermal excitation process, while a different excitation mechanism occurs in the argon and helium gas cases.

The effect of the ambient gas pressure on ionic Mg emission intensities in various gases of He, Ar, and ambient air was then examined using laser plasma with microwave (MA-LIBS). The sample employed is the same with the sample used in Fig. 3. It should be mentioned that the microwave used in this work is pulsed with the pulse width of around 400 μs. The laser energy was 5 mJ and the MW power and duration were 400 W and 800 μs, respectively. For data acquisition, the gate delay time was 1 μs and the measurement time duration was 800 μs. Fig. 4 displays the graphs how the ionic Mg intensities in He, Ar, and ambient air change with ambient pressure for (a) Mg II 280.3 nm, (b) Mg II 279.8 nm, (c) Mg II 293.6 nm, and (d) Mg II 448.1 nm. It can clearly be seen that the graphs shows almost the same profile with Fig. 3. Namely, all ionic emission intensity peaks occur at low pressure of around 1.3 kPa and their intensities then decrease with increasing the ambient pressure. However, it should be noticed that the emission intensities of all ionic emission lines increase in He, Ar, and ambient air using MA-LIBS. The microwave plays an important role in the increment of emission intensities. As reported in our previous work [49], when the microwave is introduced into the laser plasma, the electrons in the plasma region are accelerated by the electric field of the microwave radiation, increasing the kinetic energy of electron. With the kinetic energy increment, the number of collisions between electrons and other plasma constituents increases, which affects the densities of electrons, ions, and neutral atoms in the plasma, allowing the improvement of emission intensities.

It should also be noticed that the emission intensity of ionic Mg having low excitation energy of 4.4 eV is higher in Ar and He gases, and it is faintly detected in ambient air. For ionic Mg having high excitation energy of 8.7 eV (Mg II 293.6 nm) and 8.9 eV (Mg II 279.8 nm), the intensities are significantly high in He gas and very low in Ar and ambient air. For ionic Mg line having very high excitation energy of 11.6 eV, the intensity is high only in He gas, and it is negligibly week in Ar and ambient air. This interesting phenomenon cannot be explained by the model of excitation process via thermal excitation process, in which the atoms are excited in the high plasma temperature.

To understand the excitation mechanism of Mg atoms in microwave-assisted laser plasma, it is also imperative to understand the emission lifetime of ionic Mg having low and high excitation energy obtained by using LIBS with and without microwave. First, we examine the time profile of the ionic Mg emission taken by using LIBS without microwave. Fig. 5 displays time dependence of (a) Mg II 280.3 nm, (b) Mg II 279.8 nm, (c) Mg II 293.6 nm, and (d) Mg II 448.1 nm obtained from the magnesium oxide sample by using LIBS without microwave in various gases of He, Ar, and air.

It can clearly be seen that regardless of excitation energy level, all ionic Mg emission lines including Mg at 280.3 nm, 279.8 nm, 293.6 nm, and 448.1 nm as in Figs. 5(a), 5(b), 5(c), and 5(d), respectively, have almost the same profile of delay time. Namely, in He gas, the emission intensities are very high at early time and then decrease with increasing time. Furthermore, all ionic Mg has long lifetime emission up to 50 μs. On the other hand, both in Ar gas and ambient air, the emission intensities of all ionic Mg lines are very weak from initial to later stage of delay time. Also, the lifetime of the emission intensities are very short up to 5 μs. This result is the same agreement with the results reported by Muliadi et al. [61,62]. Namely, the emission lifetime of atoms is much longer in He gas environment compared to the other gas like air and nitrogen. Olenici-Craciunescu et al. also reported that in plasma jet induced in different noble gases of He, Ne, and Ar, the emission of atoms having high excitation energy only clearly be detected in the He surrounding gas [63]. We have also confirmed that the lifetime of atoms having high excitation energy such as ionic Ca II 373.7 nm (excitation energy of 6.5 eV from the ground state of the Ca^{1+} ion) is much longer in He surrounding gas than the case of nitrogen and carbon dioxide gas environment as reported here [64]. This interesting phenomenon has been explained by using the excitation model via metastable He atoms.

Time profile of ionic Mg intensities obtained from the LIBS with microwave was then examined. Fig. 6 shows how the emission intensities of ionic Mg having low excitation energy (Mg II 280.3 nm) and

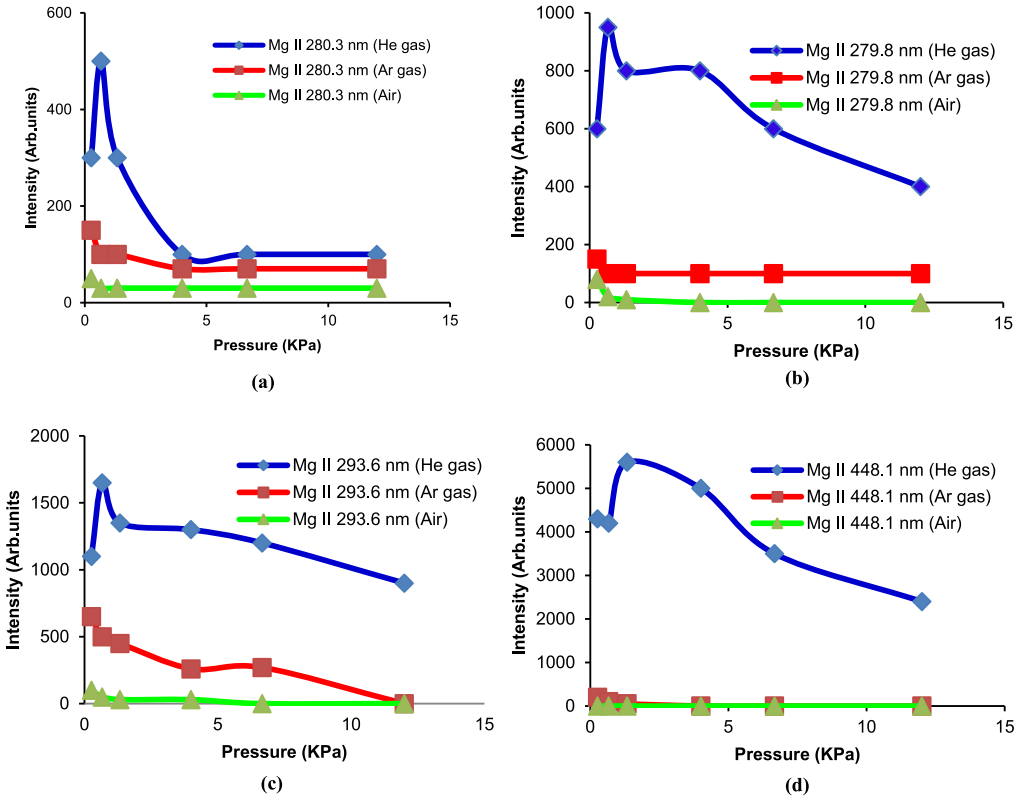

Fig. 3. Pressure dependence of (a) Mg II 280.3 nm, (b) Mg II 279.8 nm, (c) Mg II 293.6 nm, and (d) Mg II 448.1 nm taken from the magnesium oxide sample by using LIBS without microwave in various gases of He, Ar, and air.

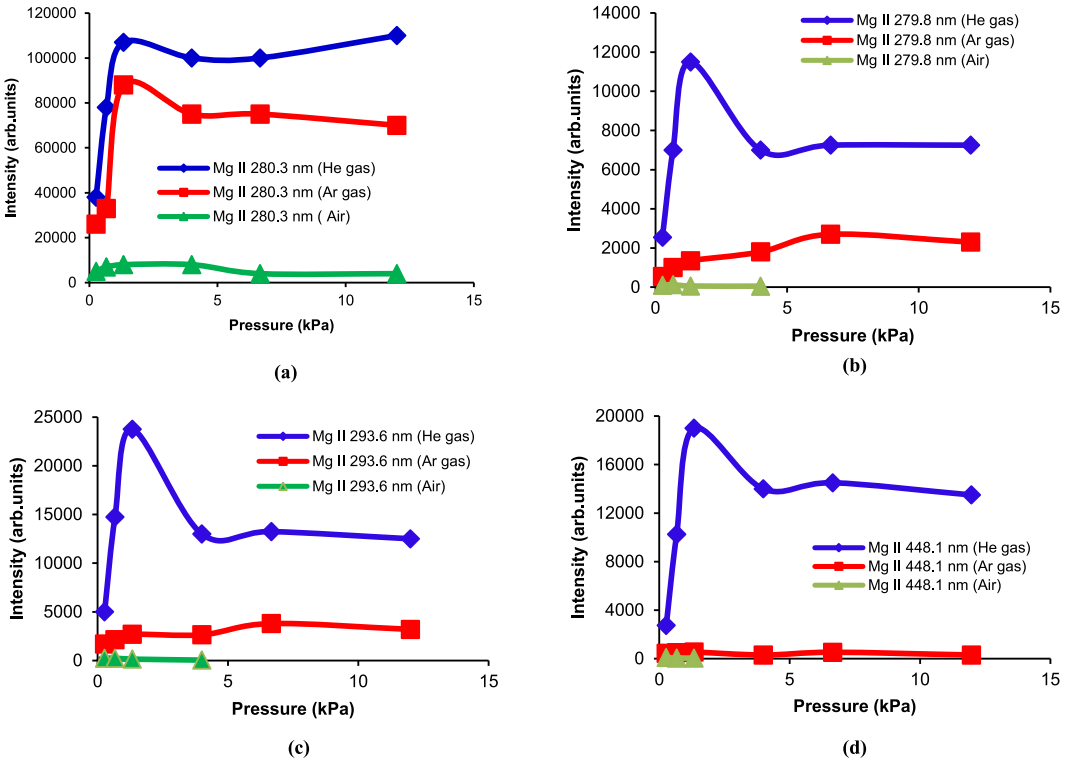

Fig. 4. Pressure dependence of (a) Mg II 280.3 nm, (b) Mg II 279.8 nm, (c) Mg II 293.6 nm, and (d) Mg II 448.1 nm taken from the magnesium oxide sample by using LIBS with microwave in various gases of He, Ar, and air.

high excitation energy (Mg II 279.8 nm, Mg II 293.6 nm, and Mg II 448.1 nm) changes with a delay time in various gases of helium, argon, and ambient air as shown in Figs. 6(a), (b), (c), and (d), respectively. Time duration of each point plotted in the graph was 5 μs. It is seen that time profile of all ionic Mg emission lines are almost the same profile with the time dependence obtained by using

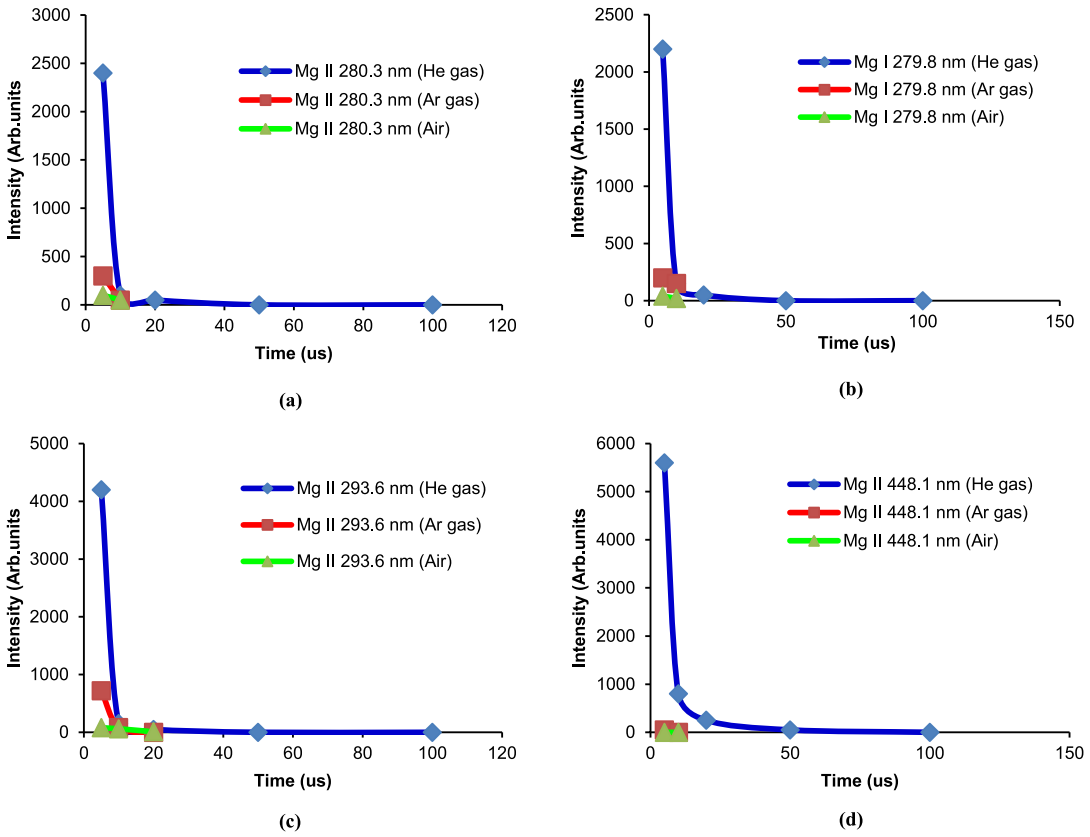

Fig. 5. Time dependence of (a) Mg II 280.3 nm, (b) Mg II 279.8 nm, (c) Mg II 293.6 nm, and (d) Mg II 448.1 nm taken from the magnesium oxide sample by using LIBS without microwave in various gases of He, Ar, and air.

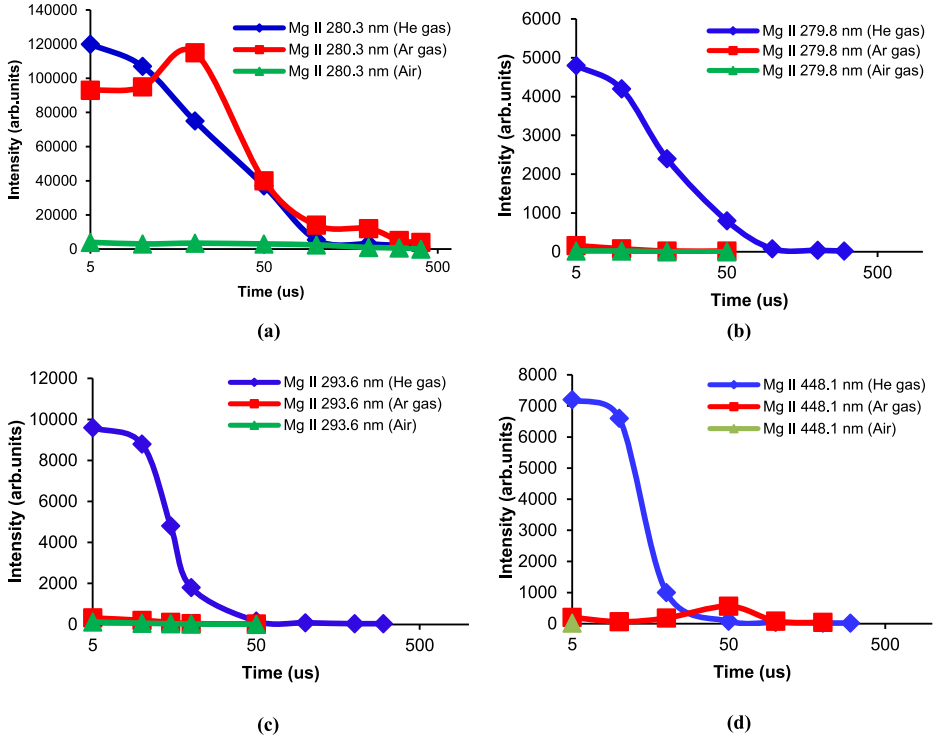

Fig. 6. Time dependence of (a) Mg II 280.3 nm, (b) Mg II 279.8 nm, (c) Mg II 293.6 nm, and (d) Mg II 448.1 nm taken from the magnesium oxide sample by using LIBS with microwave in various gases of He, Ar, and air.

LIBS without microwave as displayed in Fig. 5. Namely, in Helium gas environment, all ionic Mg lines including ionic Mg at 280.3 nm, 279.8 nm, 293.6 nm, and 448.1 nm have very high emission intensities at early stage and then the intensities decrease with increasing delay time. Furthermore, the intensity of all ionic Mg emission lines are enhanced due to the introduction of microwave radiation as explained

above. However, their intensities are relatively very weak especially in Ar gas and ambient air compared to the case of He gas, except the intensity of ionic Mg II 280.3 nm in Ar gas, which is almost the same profile with the intensity in He gas. This phenomenon cannot be explained when the excitation process taking place only by thermal process because the introduction of microwave into the laser plasma increases the plasma temperature even in ambient air as reported in our published work [49]. Nevertheless, the intensity of all ionic Mg lines is very weak in ambient air. It is supposed that in He and Ar gases, the excitation mechanism takes place through other excitation process, namely metastable atoms via penning effect.

Based on the experimental results above, it is certified that the ambient gases strongly affect the excitation process of Mg ions in the plasma region, resulting in intensity difference depending on ambient gases. This further implies that the excitation and ionization process is based on collisions with ambient gas species. As reported in some papers [61–66], plasma induced in helium and argon gases produced metastable atoms, which could become an excitation source in the laser plasma; the rare gases including helium and argon possess the metastable level states that have long lifetime compared to other levels. In this case, the amounts of energetic electrons produced in the plasma recombine with the gas species in the plasma region, producing lots of metastable atoms. The argon has metastable states at 11.55 eV and 11.72 eV, while the helium metastable state is 19.82 eV. It is assumed that the population of the metastable atoms significantly increases when the microwave was injected into the laser plasma. This is because the electrons populated in the plasma are accelerated by the electromagnetic field induced by the microwave to provide high kinetic energy, inducing the cascade ionization of gas species in the plasma region. At later stage, the electrons recombine with the ionized gas in the plasma region and excited species of metastable atoms are overwhelmingly produced. The population of metastable atoms in the microwave-assisted laser plasma is much larger compared to the case of laser plasma only because the amounts of energetic electrons and ionized gas produced in the microwave-assisted laser plasma are much plentiful. The metastable state has 10^6-10^7 longer lifetime than other states and can play an important role as an energy reservoir for exciting and ionizing other atoms through penning effect; Penning effect is the process of ionization of gas atoms or molecules by collisions with metastable atoms [65].

From the results above, we also obtained that the ionic Mg lines that have a high excitation energy (more than 8 eV from the ground state of the Mg ion) including Mg II 279.8 nm, Mg II 293.6 nm, and Mg II 448.1 nm can effectively be excited in the helium gas case. Duffendack et al. reported that the metastable helium atoms play an important role as an excitation source of magnesium ions having a high excitation energy [66]. In their research, normal low voltage arcs were maintained in mixtures of magnesium vapor with hydrogen, argon, neon and helium respectively. A similar role of He metastable atoms in excitation has also been observed by Olenici-Craciunescu et al. [63]. They reported that, by using plasma jet induced in different noble gases including He, Ne, and Ar, the emission of the N_2^+ first negative system, which has a high excitation energy, can only be detected in the He surrounding gas. In our study, we propose that the magnesium atoms are excited via metastable helium atoms overwhelmingly produced in the microwave-assisted helium plasma. It should be mentioned that in our microwave-assisted helium plasma, many metastable helium atoms are produced because the plasma has a large a diameter of approximately 15 mm. For argon gas case, it is assumed that the metastable argon atoms would not be expected as an excitation source because the ionization potential of argon and excited state of argon metastable atoms are less than the excitation potentials of these levels [66]. Further study is necessary to affirm the role of metastable helium atoms in the excitation process in microwave-assisted laser plasma.

4. Conclusions

Study on effect of ambient gas in microwave-assisted laser plasma has been carried out by using magnesium oxide sample in microwave-assisted laser-induced plasma. An intensified microwave was introduced into the LIBS plasma to enhance the plasma emission. The results certified that the ionic magnesium emission intensity varies with ambient gas kinds including helium, argon, and air. The ionic Mg line having low excitation state (Mg II 280.3 nm) clearly appears in He and Ar ambient gases, while the ionic Mg line having high excitation energy state (Mg II 279.8 nm, Mg II 293.6 nm, and Mg II 448.1 nm) can only be detected in helium microwave-assisted helium plasma. Metastable helium atoms are supposed to play an important role as an excitation energy source of magnesium emission in He gas environment.

Declaration of competing interest

The authors declare that they have no known competing financial interests or personal relationships that could have appeared to influence the work reported in this paper.

Acknowledgments

Present study includes the result of “Development of laser remote analysis for next generation nuclear fuel and applied study by MOX sample” entrusted to Japan Atomic Energy Agency by the Ministry of Education, Culture, Sports, Science and Technology of Japan (MEXT). Part of this study was financially supported by Ministry of Education and Culture, Indonesia under contract No. 225-90/UN7.6.1/PP/2020.

References

[1] L.J. Radziemski, R.W. Solarz, J.A. Paisner, Laser Spectroscopy and Its Applications, first ed., Marcel Dekker, New York, 1987.
[2] A. Miziolek, V. Palleschi, I. Schechter, Ed. Laser Induced Breakdown Spectroscopy, Cambridge University Press, 2006.
[3] L. Jolivet, M. Leprince, S. Moncayo, L. Sorbier, C.P. Lienemann, V. Motto-Ros, Review of the recent advances and applications of LIBS-based imaging, Spectrochim. Acta Part B At. Spectrosc. 151 (2019) 41–53.
[4] G. Galbács, A critical review of recent progress in analytical laser-induced breakdown spectroscopy, Anal. Bioanal. Chem. 407 (2015) 7537–7562.
[5] G.S. Senesi, N. Senesi, Laser-induced breakdown spectroscopy (LIBS) to measure quantitatively soil carbon with emphasis on soil organic carbon, A Rev. Anal. Chimica Acta 938 (2016) 7–17.
[6] S. Millar, C. Gottlieb, T. Gü, N. Sankat, G. Wilsch, S. Kruschwitz, Chlorine determination in cement-bound materials with laser-induced breakdown spectroscopy (LIBS), a review and validation spectrochim, Acta Part B At. Spectrosc. 147 (2018) 1–8.
[7] J. Moros, J. Laserna, Laser-induced breakdown spectroscopy (LIBS) of organic compounds, A Rev. Appl. Spectrosc. 73 (9) (2019) 963–1011.
[8] S.C. Jantzi, V. Motto-Ros, F. Trichard, Y. Markushin, N. Melikechi, A.D. Giacomo, Sample treatment and preparation for laser-induced breakdown spectroscopy, Spectrochim. Acta Part B: At. Spectrosc. 115 (2016) 52–63.
[9] D.F. Andrade, M.A. Sperançaa, E.R. Pereira-Filho, Different sample preparation methods for the analysis of suspension fertilizers combining LIBS and liquid-to-solid matrix conversion: determination of essential and toxic elements, Anal. Methods 9 (2017) 5156–5164.
[10] M.A. Sperança, M.S. Pomares-Alfonsob, E.R. Pereira-Filho, Analysis of cuban nickeliferous minerals by laser-induced breakdown spectroscopy (LIBS): non-conventional sample preparation of powder samples, Anal. Methods 10 (2018) 533–540.
[11] V.K. Singh, J. Sharma, A.K. Pathak, C.T. Ghany, M.A. Gondal, Laser-induced breakdown spectroscopy (LIBS): a novel technology for identifying microbes causing infectious diseases, Biophys. Reviews 10 (2018) 1221–1239.
[12] A.S. Anderson, H. Mukundan, R.E. McInroy, S.M. Clegg, Combined LIBS-Raman for remote detection and characterization of biological samples, in: Proc. SPIE 9328, Imaging, Manipulation, and Anal. of Biomol. Cells, and Tissues XIII, 2015, p. 932811.
[13] S.J. Rehse, A review of the use of laser-induced breakdown spectroscopy for bacterial classification, quantification, and identification, Spectrochim. Acta Part B: At. Spectrosc. 154 (2019) 50–69.
[14] B.B.S. Jaswal, V. Kumar, J. Sharma, P.K. Rai, M.A. Gondal, B. Gondal, V.K. Singh, Analysis of heterogeneous gallstones using laser-induced breakdown spectroscopy (LIBS) and wavelength dispersive X-ray fluorescence (WD-XRF), Lasers Med. Sci. 31 (2016) 573–579.

[15] V.K. Singh, V. Kumar, J. Sharma, Importance of laser-induced breakdown spectroscopy for hard tissues (bone, teeth) and other calcified tissue materials, Lasers Med. Sci. 30 (2015) 1763–1778.
[16] Y. Markushin, P. Sivakumar, D. Connolly, N. Melikechi, Tag-femtosecond laser-induced breakdown spectroscopy for the sensitive detection of cancer antigen 125 in blood plasma, Anal. Bioanal. Chem. 407 (2015) 1849–1855.
[17] M. Corsi, G. Cristoforetti, V. Palleschi, A. Salvetti, E. Tognoni, A fast and accurate method for the determination of precious alloys caratage by laser induced plasma spectroscopy, Eur. Phys. J. D 13 (3) (2001) 373–377.
[18] F. Ruan, T. Zhang, H. Li, Laser-induced breakdown spectroscopy in archeological science: a review of its application and future perspectives, Appl. Spectrosc. Rev. 54 (7) (2019) 573–601.
[19] S. Guirado, F.J. Fortes, J.J. Laserna, Elemental analysis of materials in an underwater archeological shipwreck using a novel remote laser-induced breakdown spectroscopy system, Talanta 137 (2015) 182–188.
[20] A.A.C. Carvalho, L.A. Cozer, M.S. Luz, L.C. Nunes, F.R.P. Rocha, C.S. Nomura, Multi-energy calibration and sample fusion as alternatives for quantitative analysis of high silicon content samples by laser-induced breakdown spectrometry, J. Anal. At. Spectrom. 34 (8) (2019) 1701–1707.
[21] G. Nicolodelli, G.S. Senesi, R.A. Romano, J. Cabral, I.L.O. Perazzoli, B.S. Marangoni, P.R. Villas-Boas, D.M.B.P. Milori, Laser-induced breakdown spectroscopy of environmental and synthetic samples using non-intensified CCD: optimization of the excitation wavelength, Appl. Phys. B 123 (2017) 127.
[22] K.Q. Yu, Y.R. Zhao, F. Liu, Y. He, Laser-induced breakdown spectroscopy coupled with multivariate chemometrics for variety discrimination of soil, Sci. Rep. 6 (2016) 27574.
[23] D. Meng, N. Zhao, Y. Wang, M. Ma, L. Fang, Y. Gu, Y. Jia, J. Liu, On-line/on-site analysis of heavy metals in water and soils by laser induced breakdown spectroscopy, Spectrochim. Acta Part B: At. Spectrosc. 137 (2017) 39–45.
[24] D.K. Tripathi, V.P. Singh, S.M. Prasad, D.K. Chauhan, A.K. Rai, Silicon-mediated alleviation of cr (VI) toxicity in wheat seedlings as evidenced by chlorophyll florescence, laser induced breakdown spectroscopy and anatomical changes, Ecotoxicol. Environ. Safety 113 (2015) 133–144.
[25] B. Bhatt, K.H. Angeyo, A.D. Kamadjeu, LIBS Development methodology for forensic nuclear materials analysis, Anal. Methods 10 (2018) 791–798.
[26] K. Subedi, T. Trejos, J. Almirall, Forensic analysis of printing inks using tandem Laser Induced Breakdown Spectroscopy and Laser Ablation Inductively Coupled Plasma Mass Spectrometry, Spectrochim. Acta Part B: At. Spectrosc. 103–104 (2015) 76–83.
[27] S. Choi, Jack, J. Yoh, Fire debris analysis for forensic fire investigation using laser induced breakdown spectroscopy, Spectrochim. Acta Part B: At. Spectrosc. 134 (2017) 75–80.
[28] D.S. Vogt, K. Rammelkamp, S. Schrö, H.W. Hü, Molecular emission in laser-induced breakdown spectroscopy: An investigation of its suitability for chlorine quantification on mars, Icarus 302 (2018) 470–482.
[29] C. Lefebvre, A. Catalá, P. Sobron, A. Koujelev, R. Lé, Depth-resolved chemical mapping of rock coatings using laser-induced breakdown spectroscopy: Implications for geochemical investigations on Mars, Planet. Space Sci. 126 (2016) 24–33.
[30] S.N. Abdulmadjid, M. Pardede, H. Suyanto, M. Ramli, K. Lahna, A.M. Marpaung, R. Hedwig, Z.S. Lie, D.P. Kurniawan, K.H. Kurniawan, T.J. Lie, N. Idris, M.O. Tjia, K. Kagawa, Evidence of feasible hardness test on Mars using ratio of ionic/neutral emission intensities measured with laser-induced breakdown spectroscopy in low pressure CO2 ambient gas, J. Appl. Phys. 119 (2016) 163304.
[31] D.F. Andrade, E.R. Pereira-Filho, Direct determination of contaminants and major and minor nutrients in solid fertilizers using laser-induced breakdown spectroscopy (LIBS), J. Agricul. and Food Chem. 64 (41) (2016) 7890–7898.
[32] D.W. Hahn, N. Omenetto, Laser-induced breakdown spectroscopy (LIBS), part II: Review of instrumental and methodological approaches to material analysis and applications to different fields, Appl. Spectrosc. 66 (4) (2012) 347–419.
[33] V.I. Babushok, F.C. DeLucia Jr, J.L. Gottfried, A.W. Miziolek, Double pulse laser ablation and plasma: Laser induced breakdown spectroscopy signal enhancement, Spectrochim. Acta Part B 61 (2006) 999–1014.
[34] J. Uebbing, J. Brust, W. Sdorra, F. Leis, K. Niemax, Reheating of a laser-produced plasma by a second pulse laser, Appl. Spectrosc. 45 (1991) 1419–1423.
[35] R. Nyga, W. Neu, Double-pulse technique for optical emission spectroscopy of ablation plasmas of samples in liquids, Opt. Lett. 18 (1993) 747–749.
[36] R. Ahmed, J. Iqbal1, M.A. Baig, Effects of laser wavelengths and pulse energy ratio on the emission enhancement in dual pulse LIBS, Laser Phys. Lett. 12 (2015) 066102.
[37] Y. Wang, A. Chen, S. Li, L. Sui, D. Liu, D. Tian, Y. Jiang, M. Jin, Enhancement of laser-induced Fe plasma spectroscopy with dual-wavelength femtosecond double-pulse, J. Anal. At. Spectrom. 31 (2016) 497–505.
[38] J.K. Antony, N.J. Vasa, V.L.N.S. Raja, A.S. Laxmiprasad, Single laser based dual-wavelength ablation technique for emission enhancement during LIBS, J. Phys. D: Appl. Phys. 45 (2012) 365401.
[39] Y. Lu, V. Zorba, X. Mao, R. Zheng, R.E. Russo, UV Fs–ns double-pulse laser induced breakdown spectroscopy for high spatial resolution chemical analysis, J. Anal. At. Spectrom. 28 (2013) 743–748.
[40] G. Cristoforetti, Orthogonal double-pulse versus single-pulse laser ablation at different air pressures: A comparison of the mass removal mechanisms, Spectrochim. Acta Part B: At. Spectrosc. 64 (1) (2009) 26–34.
[41] B.Y. Cai, X. Mao, H. Hou, V. Zorba, R.E. Russo, N.H. Cheung, Double-pulse laser ablation sampling: Enhancement of analyte emission by a second laser pulse at 213 nm, Spectrochim. Acta Part B: At. Spectrosc. 110 (2015) 51–55.
[42] L. Caneve, F. Colao, R. Fantoni, V. Spizzichino, Laser ablation of copper based alloys by single and double pulse laser induced breakdown spectroscopy, Appl. Phys. A 85 (2) (2006) 151–157.
[43] Envimetrics, LAMPS unit manual, 2009.
[44] Y. Liu, M. Baudelet, M. Richardson, Elemental analysis by microwave-assisted laser-induced breakdown spectroscopy: Evaluation on ceramics, J. Anal. At. Spectrom. 25 (2010) 1316–1323.
[45] B. Kearton, Y. Mattley, Laser-induced breakdown spectroscopy: sparking new applications, Nat. Photonics 2 (2008) 537–540.
[46] Y. Liu, B. Bousquet, M. Baudelet, M. Richardson, Improvement of the sensitivity for the measurement of copper concentrations in soil by microwave-assisted laser-induced breakdown spectroscopy, Spectrochim. Acta Part B 73 (2012) 89–92.
[47] Y. Ikeda, A. Moon, M. Kaneko, Development of microwave-enhanced spark induced breakdown spectroscopy, Appl. Opt. 49 (2010) C95–C100.
[48] Y. Ikeda, R. Tsuruoka, Characteristics of microwave plasma induced by lasers and sparks, Appl. Opt. 51 (2012) B183–B191.
[49] A. Khumaeni, M. Tampo, K. Akaoka, M. Miyabe, I. Wakaida, Enhancement of LIBS emission using antenna-coupled microwave, Opt. Express 21 (2013) 29755–29768.
[50] Effenberger Jr. A.J., J.R. Scott, Effect of atmosphere on collinear double-pulse laser-induced breakdown spectroscopy, Anal. Bioanal. Chem. 400 (2011) 3217–3227.
[51] A.J. Effenberger Jr, J.R. Scott, Effect of atmospheric conditions on LIBS spectra, Sensors 10 (5) (2010) 4907–4925.
[52] A. Bogaerts, Z.Y. Chen, D. Bleiner, Laser ablation of copper in different background gases: comparative study by numerical modeling and experiments, J. Anal. At. Spectrom. 21 (4) (2006) 384–395.
[53] W. Sdorra, K. Niemax, Basic investigations for laser microanalysis 3: Application of different buffer gases for laser produced sample plumes, Microchim. Acta 107 (3–6) (1992) 319–327.
[54] N. Idris, M. Pardede, E. Jobiliong, Z.S. Lie, R. Hedwig, M.M. Suliyanti, D.P. Kurniawan, K.H. Kurniawan, K. Kagawa, M.O. Tjia, Enhancement of carbon detection sensitivity in laser induced breakdown spectroscopy with low pressure ambient helium gas, Spectrochim. Acta Part B: Atomic Spectrosc. 151 (2019) 26–32.
[55] R. Hedwig, K. Lahna, R. Idroes, I. Karnadi, I. Tanra, J. Iqbal, D. Kwaria, D.P. Kurniawan, K.H. Kurniawan, M.O. Tjia, K. Kagawa, Food analysis employing high energy nanosecond laser and low pressure He ambient gas, Microchem. J. 147 (2019) 356–364.
[56] A. Khumaeni, Z.S. Lie, Y.I. Lee, K. Kurihara, K.H. Kurniawan, K.I. Fukumoto, K. Kagawa, H. Niki, Emission characteristics of Ca and mg atoms in gas plasma induced by the bombardment of transversely excited atmospheric CO2 laser at 1 atm, Japan. J. Appl. Phys. 51 (2012) 082403.
[57] Atomic line Data (R.L. Kurucz and B. Bell) Kurucz CD-ROM (23) Cambridge, Mass.: Smithson ian Astrophysical Observatory, 1995, http://www.cfa.harvard.edu/amp/ampdata/kurucz23/sekur.html.
[58] http://physics.nist.gov/PhysRefData/ASD/lines_form.html.
[59] S. Bashir, N. Farid, K. Mahmood, M.S. Rafique, Influence of ambient gas and its pressure on the laser-induced breakdown spectroscopy and the surface morphology of laser-ablated cd, Appl. Phys. A 107 (2012) 203–212.
[60] K. Knight, N.L. Scherbarth, D.A. Cremers, M.J. Ferris, Characterization of laser-induced breakdown spectroscopy (LIBS) for application to space exploration, Appl. Spectrosc. 54 (2000) 331–340.
[61] M. Ramli, N. Idris, K. Fukumoto, H. Niki, F. Sakan, T. Maruyama, K.H. Kurniawan, T.J. Lie, K. Kagawa, Hydrogen analysis in solids samples by utilizing metastable helium atoms induced by TEA CO_2 laser plasma helium gas at 1 atmosphere, Spectrochim. Acta Part B 62 (2007) 1379–1389.
[62] M. Ramli, K. Kagawa, S.N. Abdulmadjid, N. Idris, W.S. Budi, M.A. Marpaung, K.H. Kurniawan, T.J. Lie, M.M. Suliyanti, R. Hedwig, M. Pardede, Z.S. Lie, M.O. Tjia, Some notes on the role of meta-stable excited state of helium atom in laser-induced helium gas breakdown spectroscopy, Appl. Phys B 86 (2007) 729–734.
[63] S.B. Olenici-Craciunescu, A. Michels, C. Meyer, R. Heming, S. Tombrink, W. Vautz, J. Franzke, Characterization of a capillary dielectric barrier plasma jet for use as a soft ionization source by optical emission and ion mobility spectrometry, Spectrochim. Acta, Part B 64 (2009) 1253–1258.
[64] A. Khumaeni, Z.S. Lie, Y.I. Lee, K. Kurihara, K.H. Kurniawan, K. Fukumoto, K. Kagawa, H. Niki, Emission characteristics of Ca and mg atoms in gas plasma induced by the bombardment of transversely excited atmospheric CO_2 laser at 1 atm, Japanese J. Appl. Phys. 51 (2012) 082403.
[65] Sahin, Tapan, E.N. Ozmutlu, R. Veenhof, Penning transfer in argon-based gas mixtures, J. Instrum. 5 (2010) 1–30.
[66] S. Duffendack, C.L. Henshaw, M. Goyer, The excitation of the Mg II spectrum by impacts metastable atoms and ions of the rare gases, Phys. Rev. 34 (1929) 1132–1137.